Journal of Pharmaceutical Analysis 13 (2023) 1365–1373

Contents lists available at ScienceDirect

Journal of Pharmaceutical Analysis

journal homepage: www.elsevier.com/locate/jpa

Original article

DMMIC derivatization-assisted liquid chromatography-mass spectrometry method for metabolite profiling of the glutathione anabolic pathway in esophageal cancer tissues and cells

Li Liu [a, b, 1], Yu-Han Lu [a, c, 1], Min-Dan Wang [a], Qun-Fei Zhao [a], Xiu-Ping Chen [a, ***], Hang Yin [b, ****], Chen-Guo Feng [a, **], Fang Zhang [a, *]

[a] The Research Center of Chiral Drugs, Shanghai Frontiers Science Center for TCM Chemical Biology, Innovation Research Institute of Traditional Chinese Medicine, Shanghai University of Traditional Chinese Medicine, Shanghai, 201203, China
[b] Department of Thoracic Surgery, Renji Hospital, School of Medicine, Shanghai Jiaotong University, Shanghai, 200127, China
[c] School of Public Health, Shanghai University of Traditional Chinese Medicine, Shanghai, 201203, China

ARTICLE INFO

Article history:
Received 24 April 2023
Received in revised form
12 August 2023
Accepted 22 August 2023
Available online 22 September 2023

Keywords:
Glutathione anabolic pathway
Metabolite profiling
DMMIC derivatization
LC-MS
Esophageal squamous cell carcinoma
p-Hydroxycinnamaldehyde
KYSE-150cell

ABSTRACT

In this work, a new pyrylium derivatization-assisted liquid chromatography-mass spectrometry (LC-MS) method was developed for metabolite profiling of the glutathione anabolic pathway (GAP) in cancer tissues and cells. The pyrylium salt of 6,7-dimethoxy-3-methyl isochromenylium tetrafluoroborate (DMMIC) was used to label the amino group of metabolites, and a reductant of dithiothreitol (DTT) was employed to stabilize the thiol group. By combining DMMIC derivatization with LC-MS, it was feasible to quantify the 13 main metabolites on the GAP in complex biological samples, which had good linearity (R^2 = 0.9981–0.9999), precision (interday precision of 1.6%–19.0% and intraday precision of 1.4%–19.8%) and accuracy (83.4%–115.7%). Moreover, the recovery assessments in tissues (82.5%–107.3%) and in cells (98.1%–118.9%) with GSH-^{13}C2, ^{15}N, and Cys-^{15}N demonstrated the reliability of the method in detecting tissues and cells. Following a methodological evaluation, the method was applied successfully to investigate difference in the GAP between the carcinoma and para-carcinoma tissues of esophageal squamous cell carcinoma (ESCC) and the effect of *p*-hydroxycinnamaldehyde (CMSP) on the GAP in KYSE-150 esophageal cancer cells. The results demonstrate that the developed method provides a promising new tool to elucidate the roles of GAP in physiological and pathological processes, which can contribute to research on drugs and diseases.

1. Introduction

Glutathione is an endogenous component of cellular metabolism, and is a tripeptide composed of glycine, cysteine, and glutamic acid [1]. Many studies have shown that glutathione is involved in various biological functions due to its anabolic pathway [2–4]; in addition, glutathione is associated with the progression of many human diseases, including aging diseases [5,6], cystic fibrosis [7,8], cardiovascular diseases [9], inflammatory diseases [10,11], immune diseases [12], metabolic diseases [13], neurodegenerative diseases [14–16], and cancers [17,18]. In particular, the glutathione anabolic pathway (GAP) plays a dual role in the development of cancers [19,20]. GAP can remove and detoxify carcinogens, but high expression of GAP may protect cancer cells by conferring resistance to some drugs [21,22]. Targeting GAP is a potential strategy to induce cancer cell death [22,23]. Therefore, monitoring the metabolite profiling of GAP is of great importance and contributes to research on drugs and diseases.

There are 13 main metabolites in the GAP (Fig. 1), namely, glutamine (Gln), glutamic acid (Glu), glycine (Gly), serine (Ser), methionine (Met), S-adenylyl homocysteine (SAH), O-acetyl-serine (OAS), homocysteine (HCys), cystathionine (Cysta), cysteine (Cys), cysteinylglycine (CG), glutamylcysteine (GC), and glutathione (GSH). In terms of chemical structure, some of these metabolites

Peer review under responsibility of Xi'an Jiaotong University.
* Corresponding author.
** Corresponding author.
*** Corresponding author.
**** Corresponding author.
E-mail addresses: xiupingchen@shutcm.edu.cn (X.-P. Chen), yinhang@renji.com (H. Yin), fengcg@shutcm.edu.cn (C.-G. Feng), fzhang@shutcm.edu.cn (F. Zhang).
[1] Both authors equally contributed to this work.

https://doi.org/10.1016/j.jpha.2023.08.016

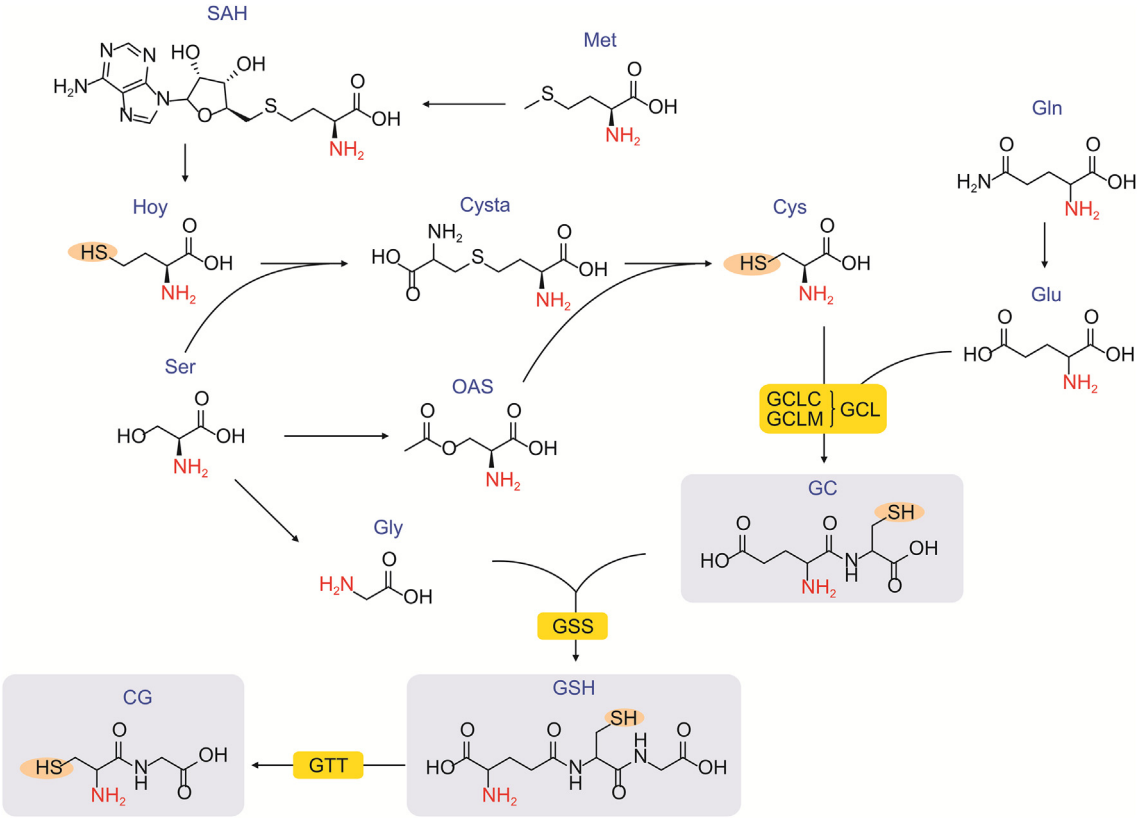

Fig. 1. Glutathione anabolic pathway (GAP). Gln: glutamine; Ser: L-serine; Gly: L-glycine; GC: glutamylcysteine; SAH: S-adenylyl homocysteine; Glu: L-glutamine; CG: cysteinylglycine; OAS: O-acetyl-serine; Cys: L-cysteine; Cysta: cystathionine; Hcys: homocysteine; Met: L-methionine; GSH: glutathione; GTT: γ-glutamyl transferase; GSS: glutathione synthetase; GCLM: glutamate-cysteine ligase modifier subunit gene; GCLC: glutamate-cysteine ligase catalytic subunit gene.

contain thiol groups while others contain small-molecule oligopeptides; thus, analysis can be difficult because these compounds exhibit chemical instability, are highly polar, are not very abundant and easily undergo enzymatic hydrolysis. Thus, many efforts have been dedicated to achieving efficient, sensitive, and accurate analysis [24]. Among them, the enzymatic recycling assay [25] is a classic approach that can quantitatively determine glutathione. However, the amount of enzyme used is large and costly, and its good specificity cannot be used to simultaneously detect other metabolites in the pathway. As a new technology, fluorescent probes have also been reported to be an ideal tool for the real-time monitoring of glutathione [26,27]. However, similar to the enzymatic recycling assay, fluorescent probes cannot cover metabolites with different structures in the pathway [28]. Compared with these methods, liquid chromatography-mass spectrometry (LC-MS) is a preferred tool for metabolite profiling due to its good selectivity, sensitivity, and high-coverage [29,30]. In particular, with the assistance of chemical derivatization [31,32], LC-MS has greatly improved the analysis of compounds that contain unstable functional groups, exhibit large polarity, show no chromatographic retention, and exhibit poor MS ionization.

In previous studies, it was demonstrated that an effective pyrylium salt [33] named 6,7-dimethoxy-3-methyl isochromenylium tetrafluoroborate (DMMIC) could greatly improve the quantification of amino compounds (ACs) when combined with LC-MS (Fig. 2). Considering that the 13 metabolites involved in GAP each contain an amino group, the aim of this study is to exploit the advantages of DMMIC combined with LC-MS to realize metabolite profiling. In addition, to stabilize the metabolites containing the thiol group, a reductant of dithiothreitol (DTT) was added to the sample pretreatment; the power and effect of DTT on the subsequent derivation and detection were investigated. Finally, the developed method was evaluated using a systematic methodology and applied to investigate the difference in the GAP between carcinoma and para-carcinoma tissues of esophageal squamous cell carcinoma (ESCC). Furthermore, the effect of *p*-hydroxycinnamaldehyde (CMSP) on the GAP in KYSE-150 esophageal cancer cells was evaluated.

2. Materials and methods

2.1. Reagents

The synthesis of [d_0]-/[d_3]-DMMIC was performed in-house according to a previously reported method [33]. L-glycine (Gly), glutamine (Gln), and L-glutamine (Glu) were purchased from Aladdin (Shanghai, China). L-serine (Ser), L-methionine (Met), formic acid, L-cysteine-^{15}N (Cys-^{15}N) and glutathione-^{13}C2, ^{15}N (GSH-^{13}C2, ^{15}N) sodium salt were purchased from J&K Scientific (Beijing, China). Hydrochloric acid (HCl), L-cysteine (Cys) and DL-homocysteine (HCys) were purchased from Sinopharm Group Co., Ltd. (Shanghai, China). *p*-Hydroxycinnamaldehyde (CMSP) was purchased from JiuDing (Shanghai, China). Cysteinylglycine (CG), glutamylcysteine (GC), and glutathione (GSH) were purchased from

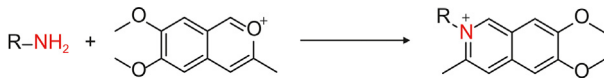

Fig. 2. Reaction of 6,7-dimethoxy-3-methyl isochromenylium tetrafluoroborate (DMMIC) with amines.

BiDe (Shanghai, China). O-acetyl-serine (OAS) and cystathionine (Cysta) were purchased from Macklin (Shanghai, China). 2-Chlorophenylalanine, dichloromethane, and phosphate buffered solution (PBS) solution were purchased from Adamas Life (Shanghai, China). Pyridine was purchased from Acros Organics (Geel, Belgium). Dithiothreitol (DTT) was procured from Beyotime (Shanghai, China) and the Cell Counting Kit-8 (CCK8) was procured from MeiLun Biotechnology (Shanghai, China). Acetonitrile and methanol of HPLC grade were purchased from Merck KGaA (Darmstadt, Germany). Deionized water was produced by a Millipore Direct Q water purification system (El Paso, TX, USA). All other chemicals and solvents used were of analytical grade. Stock solutions of standards were prepared in deionized water with 20 mM DTT at a concentration of 0.1 mol/L. Working solutions were obtained by mixing and diluting the stock solutions.

2.2. Collection and extraction of tissues and cells

2.2.1. Tissues

Tissue samples were collected from the esophagus of 10 patients with esophageal squamous at Shanghai Renji Hospital, conducted with the approval of the corresponding regulatory agencies (Approval number: No. 2021-931-06-01). The patients were informed of the objectives of the project. The tissue samples were collected immediately after surgery, frozen in liquid nitrogen, and stored at −80 °C until analysis. Before DMMIC derivatization, the frozen tissue samples were washed with ice-cold PBS solution and homogenized at 2 μL/mg in an aqueous solution containing 20 mM DTT and 10 μM 2-chlorophenylalanine. Subsequently, the homogenate was centrifuged for 3 min at 10,000 rpm, and 3 μL/mg extract was added and homogenized again. The supernatant was diluted with 4 vol of methanol to precipitate the protein. After the mixture was frozen overnight at −20 °C, the supernatant was transferred for derivatization.

2.2.2. Cells

KYSE-150 cells (4×10^5) were seeded in a 6-well plate. Cells were divided into the following groups: the Con and CMSP groups. After incubation overnight, the cells of the CMSP group were treated with 2 mL of 200 μM CMSP solution in culture medium. Blank culture medium was added to the control group. Twenty-four hours later, the culture medium was fully aspirated, and the cells were washed twice with 1 mL of PBS solution. Then, the cells were digested with 500 μL of trypsin and washed with PBS three times. Fifty microliters of 80% methanol aqueous solution containing DTT and 2-chlorophenylalanine was quickly added as the extraction and quenching solvent to the cell precipitates. The samples were repeatedly subjected to freeze–thaw cycles in liquid nitrogen and ultrasonicated 3 times, and then the extracts were stored at −80 °C until metabolic profile analysis.

2.3. DMMIC derivatization

For DMMIC derivatization, a 20 μL aliquot of the standard solution or cell and tissue extract was added to 10 μL of [d_0]- or [d_3]-DMMIC reagent (250 mM) and 70 μL of pyridine in methanol (1%). The mixture was vortexed and incubated at 50 °C for 1 h at 1000 rpm. Then, the mixture was dried by a stream of nitrogen, and the residue was dissolved in 100 μL of an aqueous solution containing 10 mM DTT and 1% HCl. The [d_0]-/[d_3]-DMMIC derivatized samples were mixed at a ratio of 1:1 (*V*/*V*). The solution was centrifuged for 3 min at 10,000 rpm, and the supernatant was used for LC-MS analysis.

2.4. LC-MS analysis

The liquid chromatography quadrupole time-of-flight mass spectrometry (LC-QTOF MS) measurements were performed on an instrument consisting of a 1290 HPLC system and a 6545 UHD quadrupole time of flight mass spectrometer (Agilent Technologies, Santa Clara, CA, USA). LC separation was carried out on a Waters XSelect HSS T3 column (2.1 mm × 150 mm, 2.5 μm; Waters, Milford, MA, USA). The mobile phase was composed of 0.4% formic acid in water (A) and MeOH (B). The profile of gradient elution was as follows: 0–1 min, 90% A; 1–2 min, 90%–70% A; 2–7 min, 70%–65% A; 7–10 min, 65%–5% A; 10–13.5 min, 5%–5% A; 13.5–14 min, 5%–90% A; and 13.5–18 min, 90% A. The column temperature was maintained at 40 °C, the flow rate was 0.3 mL/min, and the sample injection volume was 1 μL. The QTOF MS was operated with a jet stream electrospray ionization (ESI) source in positive mode. The ESI capillary voltage was set to 2500 V, the nozzle voltage was set to 0 V, and the fragment voltage was 150 V. The nitrogen drying gas flow was heated to 325 °C at a flow rate of 13 L/min. The sheath gas temperature was 350 °C at a flow rate of 12 L/min. The nebulizer was 40 psig. The mass scan range of the primary MS was *m/z* 100–1000. Before measurements were performed, the QTOF MS instrument was calibrated externally using a series of standards (*m/z* 100 − 3200) to ensure that the mass accuracy was less than 2 ppm and the mass resolution was 25,000 (*m/z* 322).

2.5. Data processing and statistical analysis

Agilent MassHunter Acquisition B.08.00 (Agilent Technologies) was used for the control of the equipment and acquisition of data. MassHunter Qualitative Analysis Navigator B.08.00 and MassHunter Quantitative Analysis B.08.00 (Agilent Technologies) were used for data processing. Orthogonal partial least squares-discriminant analysis (OPLS-DA), boxplot, heatmap and receiver operating characteristic (ROC) curves were generated using MetaboAnalyst 5.0 (http://www.metaboanalyst.ca/). All quantitative data in this study are expressed as the mean ± standard deviation (SD). Differences were evaluated by an unpaired *t*-test. $P < 0.05$ was recognized as statistically significant.

3. Results and discussion

3.1. Optimization of sample pretreatment

The stability of target metabolites is an important consideration when establishing a method to profile GAP. Cys, HCys, and other thiol metabolites are easily oxidized, while GC, CG, and GSH are vulnerable to hydrolysis by enzymes. Thus, the method used to pretreat thawed tissues was investigated at the beginning of this work; for example, the effect of freeze-drying and the addition of a reductant of DTT were examined [34]. As shown in Fig. 3, between freeze-drying groups (Figs. 3A and B), HCys, CG, GC, and SAH were successfully detected, and the signal of Cys was increased 2–3 orders of magnitude when the samples was homogenized with DTT aqueous solution compared to homogenization with water. This indicated that the addition of DTT exerted a positive effect, which reduced the disulfide bonds and ensured that the thiol groups were in a stable state, as previously reported [35,36]. However, Cysta and GSH were not detected regardless of whether DTT was added during homogenization. The molecular structure of the two metabolites might undergo irreversible degradation during the freeze-drying process. When thawed tissues were not freeze-dried but subjected to subsequent treatments directly (Figs. 3C and D), all 13 target metabolites were successfully detected in the presence of DTT, especially Cysta and GSH. Therefore, directly homogenizing tissue samples with an aqueous solution

containing DTT after thawing is the preferred pretreatment method for profiling the GAP. Normally, freeze-drying tissue can effectively eliminate the interference of its moisture on subsequent quantitative results. Considering this factor, an internal standard of 2-chlorophenylalanine was added during homogenization and its signal was used to normalize the target signals among different tissue samples during data processing.

3.2. Optimization of DMMIC derivatization

Because of the reductant DTT was used in the pretreatment, the effect of its presence on DMMIC derivatization was investigated. Five sulfhydryl-free metabolites were used as the test compounds; these metabolites were dissolved in DTT aqueous solution and water, and then underwent derivatization. Surprisingly, all DMMIC derivatives from the DTT group were higher than those from the water group, and Gln, Ser, Gly, Glu and Met were increased by 33%, 31%, 23%, 25% and 51%, respectively (Fig. 4). This result indicated that the presence of DTT exerted a certain positive impact on the derivative reaction. It was speculated that DTT might have a catalytic effect on the reaction, improving the reaction efficiency by forming active intermediates with the DMMIC reagent.

It was previously demonstrated that the following key factors affected the efficiency of the reaction: reaction temperature, reaction time, and the amount of pyridine in the DMMIC derivatization [33]. Considering the addition of DTT in this study, the reaction conditions were re-optimized by varying the concentrations of pyridine methanol solution (0, 0.5%, 1% and 1.5%), reaction times (1, 2, 3 and 4 h), and reaction temperatures (40, 50, 60 and 70 °C). Overall, the test metabolites tended to increase and then decrease with prolonged reaction time, especially for Gly and Cys. The reaction time in the range evaluated showed no obvious effect on the DMMIC derivative. The addition of pyridine did benefit the reaction, but no effect was observed within 0.5%–1.5% pyridine methanol solution. Finally, a 1% pyridine methanol solution was selected. The reaction temperature and time were maintained at 50 °C and 1 h, respectively (Fig. S1). The results obtained indicate that the DMMIC derivatization reaction was achieved under milder

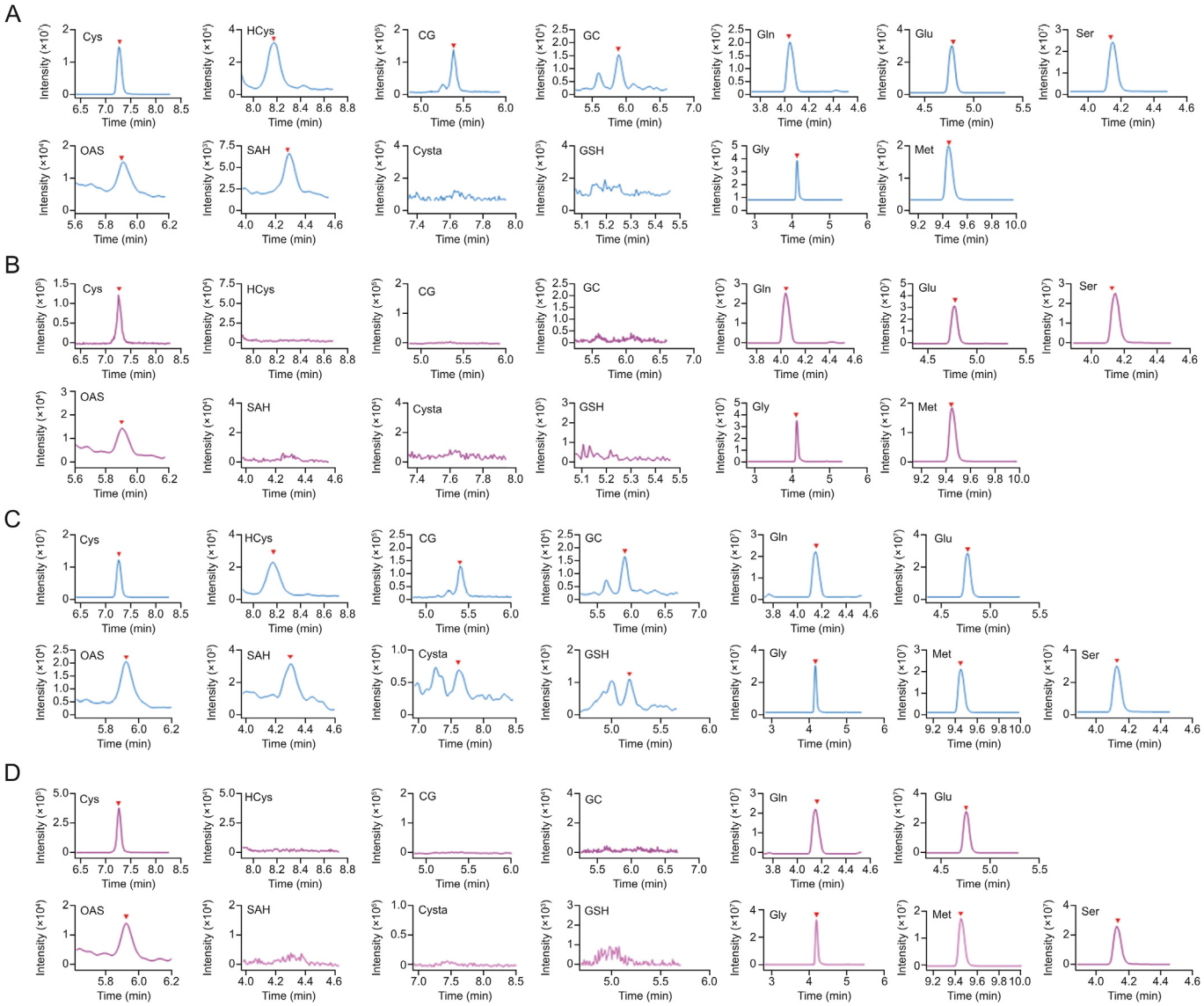

Fig. 3. Chromatograms for the metabolites in thawed tissue pretreated by (A) freeze-drying followed by homogenization with dithiothreitol (DTT) aqueous solution, (B) freeze-drying followed by homogenization with water, (C) homogenization with DTT aqueous solution, and (D) homogenization with water. Gln: glutamine; Ser: L-serine; Gly: L-glycine; GC: glutamylcysteine; SAH: S-adenylyl homocysteine; Glu: L-glutamine; CG: cysteinylglycine; OAS: O-acetyl-serine; Cys: L-cysteine; Cysta: cystathionine; Hcys: homocysteine; Met: L-methionine; GSH: glutathione.

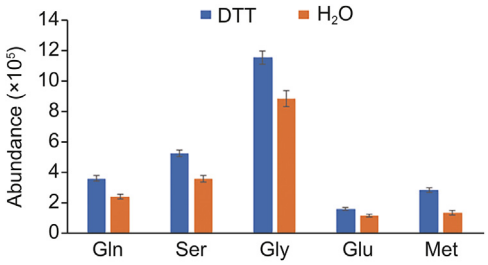

Fig. 4. Comparison of the derivatized metabolites in the 6,7-dimethoxy-3-methyl isochromenylium tetrafluoroborate (DMMIC) reaction using dithiothreitol (DTT) solution and water as solvents. Gln: glutamine; Ser: L-serine; Gly: L-glycine; Glu: L-glutamine; Met: L-methionine.

conditions with a faster kinetic reaction. After the reaction, the solution was dried with nitrogen gas to remove the pyridine, preventing the ionization of LC-MS detection from incurring interferences. For the residue, an aqueous solution containing 10 mM DTT and 1% hydrochloric acid was the preferred redissolved solvent (Fig. S2), which helped stabilize the DMMIC derivatives in the form of organic salt and replenish the DTT lost during drying with nitrogen. In addition, it was observed that extracting the redissolved solution with dichloromethane helped to remove the liposoluble impurities caused by the biologic matrix and DMMIC derivatization and increased the signals of the derivatized metabolites.

3.3. Methodology evaluation of DMMIC derivatization-assisted LC–MS

3.3.1. Linearity, limit of detection, and limit of quantification

Before the methodology evaluation, the composition of the mobile phase was evaluated for the LC–MS detection of DMMIC-derivatized metabolites. The results showed that 0.4% formic acid water and methanol could elute the derivatized metabolites well (Figs. S3 and S4). As shown in Figs. 5 and S5, under the optimal conditions, all test derivatized metabolites in tissues and cells exhibited satisfactory chromatographic behavior with good peak shapes and chromatographic retentions.

To study the feasibility of the method for linearity, a series of 12 mixed standard solutions of metabolites (SAH was

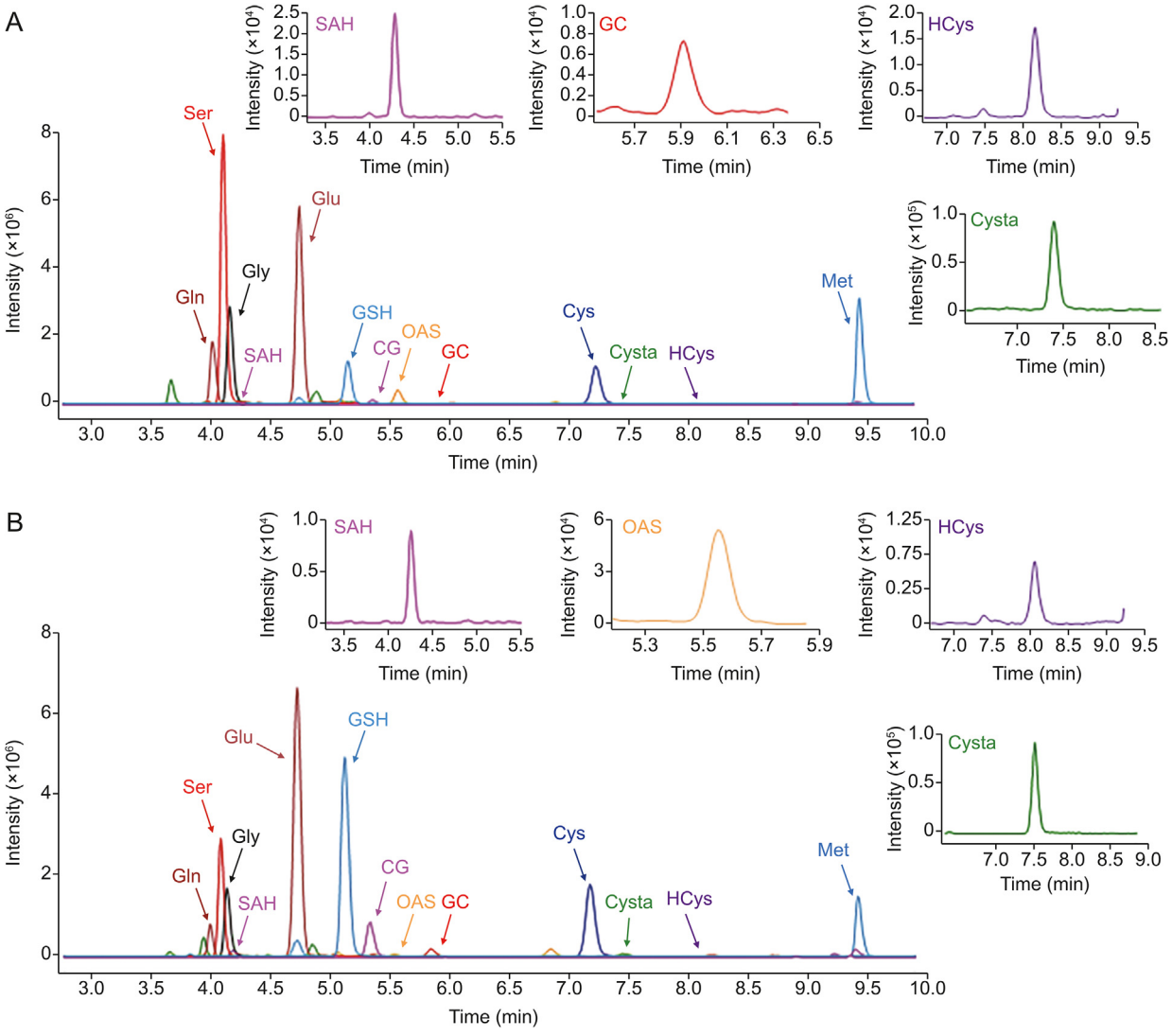

Fig. 5. The multi-extracted ionchromatograms (mEICs, *m/z* at molecular masses) of 6,7-dimethoxy-3-methyl isochromenylium tetrafluoroborate (DMMIC)-derivatized metabolites detected by liquid chromatography-mass spectrometry (LC-MS) from (A) esophageal cancer tissue and (B) KYSE-150 cells. Gln: glutamine; Ser: L-serine; Gly: L-glycine; GC: glutamylcysteine; SAH: S-adenylyl homocysteine; Glu: L-glutamine; CG: cysteinylglycine; OAS: O-acetyl-serine; Cys: L-cysteine; Cysta: cystathionine; Hcys: homocysteine; Met: L-methionine; GSH: glutathione.

uncommerciable) with different concentrations were prepared by [d_0]-DMMIC labeling and detected by LC-MS. The [d_3]-DMMIC derivatized standard solutions were used as internal standards (ISs). The calibration curve was constructed by plotting the ratio of the abundance of [d_0]-DMMIC-derivatized samples to that of IS at different concentrations. As shown in Fig. 6 and Table S1, all metabolites were confirmed to exhibit good linearity (R^2 = 0.9981–0.9999) and accuracy (83.4%–115.7%) in a concentration range of 0.05–1 μM. As the peak signal consists of at least 7 and 15 MS spectra, the concentration corresponding to the signal-to-noise (S/N) ratio ≥3 and 10 peak signals was used as the limit of detection (LOD) and limit of quantification (LOQ), respectively. The LODs and LOQs of the compounds are shown in Table S1. The LOQs were 0.5 nM for Gly, Gln, Ser and Cys, 1 nM for OAS; 2 nM for CG, 5 nM for Glu and HCys, and 10 nM for Met, and the LOQs of GSH, Cysta and GC were 50 nM. Inevitably, SAH was omitted here in the methodology evaluation due to the lack of reference standard, but assessment of the other 12 target metabolites, especially HCys owning a certain structural similarity to SAH, could demonstrate whether the developed method meets the quantitative requirements and is used for metabolite profiling of GAP including the relative quantitative analysis of SAH.

3.3.2. Stability, precision, and accuracy

Additional work, including stability, precision, and accuracy, was performed to validate the method. The stability of the DMMIC-derivatized metabolites was investigated by using the [d_3]-DMMIC-derivatized metabolites as the ISs of the [d_0]-DMMIC-derivatized. As shown in Fig. S6, the tested DMMIC-derivatized metabolites exhibited satisfactory stability over 48 h. The inter- and intra-day precision was evaluated by examining mixed standard solutions at low, medium, and high concentrations. The inter-day precision was 1.6%–19.0%, and the intra-day precision was 1.4%–19.8% (Table S1).

To verify the accuracy of the metabolic profile analysis method in tissue and cell samples, two recovery assessments were investigated using GSH-^{13}C2,^{15}N and Cys-^{15}N (for details, see supporting information) at low, medium and high concentrations (100, 500 nM, and 1 μM). As shown in Table 1 and Fig. S7, the recoveries at different concentrations ranged from 82.5% to 107.3% for tissue and 98.1%–118.9% for cells. These results indicated that the developed method could be used to perform accurate quantitative analysis of metabolites in tissue and cell samples.

3.4. Applications of metabolite profiling in tissues and cells

3.4.1. Difference in the GAP between the carcinoma and para-carcinoma tissues of ESCC

Esophageal cancer is among the most common cancers worldwide, causing hundreds of thousands of deaths each year [37]. Studies have shown that the concentration of glutathione in esophageal cancer is abnormal [38]. To investigate the difference in the GAP between the carcinoma and para-carcinoma tissues of ESCC, thirteen metabolites were detected, and their relative quantification was carried out (Fig. S8).

In the OPLS-DA model, significant differences were found in the GAP between the carcinoma and para-carcinoma tissues of ESCC with variable importance in projection (VIP) values of 7 metabolites (Glu, Cys, Gly, HCys, Ser, CG, and Met) greater than 1 (Fig. 7A). The heatmap showed that GAP was highly expressed in carcinoma tissues (Fig. 7B). Moreover, the 7 metabolites with significant differences were confirmed using box diagrams (Fig. S9). Except for CG, the expression of the remaining 6 metabolites in cancer tissues was significantly higher than that in para-cancerous tissues. ROC curve analysis showed that the area under curve (AUC) values of the six metabolites were greater than 0.7, which further indicated that Gly, Glu, Met, Ser, HCys, and Cys were significantly up-regulated in carcinoma tissues (Fig. S10).

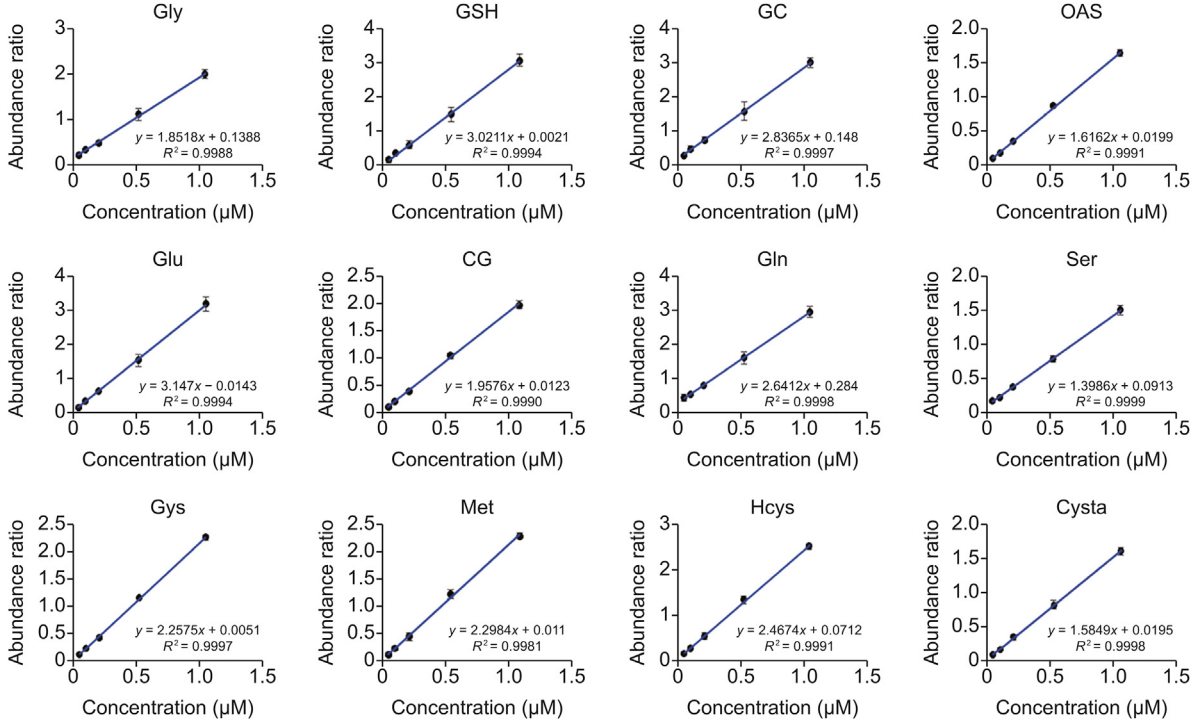

Fig. 6. Calibration curves of the 6,7-dimethoxy-3-methyl isochromenylium tetrafluoroborate (DMMIC)-derivatized metabolites. Gln: glutamine; Ser: L-serine; Gly: L-glycine; GC: glutamylcysteine; Glu: L-glutamine; CG: cysteinylglycine; OAS: O-acetyl-serine; Cys: L-cysteine; Cysta: cystathionine; Hcys: homocysteine; Met: L-methionine; GSH: glutathione.

Table 1
Recovery assessment of 6,7-dimethoxy-3-methyl isochromenylium tetrafluoroborate (DMMIC)-derivatized metabolites in tissues and cells.

Compound	Linear equation	R^2	Linear rang (μM)	Tissue recovery (%)[a,c]			Cell recovery (%)[a,c]		
				Low[b]	Middle[b]	High[b]	Low[b]	Middle[b]	High[b]
GSH-$^{13}C2,^{15}N$	y = 2.6543x − 0.0584	0.9992	0.1–2.0	107.3	104.8	96.2	114.7	101.4	100.4
Cys-^{15}N	y = 2.1909x + 0.0115	0.9998	0.1–2.0	90.6	88.4	82.5	118.9	108.9	98.1

[a] Recovery (%)=(the metabolites measured)/(the metabolites added) × 100%.
[b] Low/middle/high concentration of added standard solution at 100 nM/500 nM/1 μM, respectively.
[c] Calculated with six replicates.

3.4.2. *Effect of CMSP on GAP in KYSE-150 esophageal cancer cells*

Momordica cochinchinensis (Lour.) Spreng., commonly known as Gac fruit, is a perennial dioecious cucurbit plant that originated in South and Southeast Asia and is widely sold for dietary and medicinal purposes. Reportedly, *Momordica cochinchinensis* can effectively inhibit the growth of cancer cells, such as gastric cancer, liver cancer, and esophageal cancer cells [39]. CMSP, as an important active component of *Momordica cochinchinensis*, has been reported to affect NF-κB signaling pathways [40], which are closely related to the expression of glutathione. Thus, we conducted a study on the effect of CMSP intervention on GAP in esophageal cancer cells (Figs. S11 and S12).

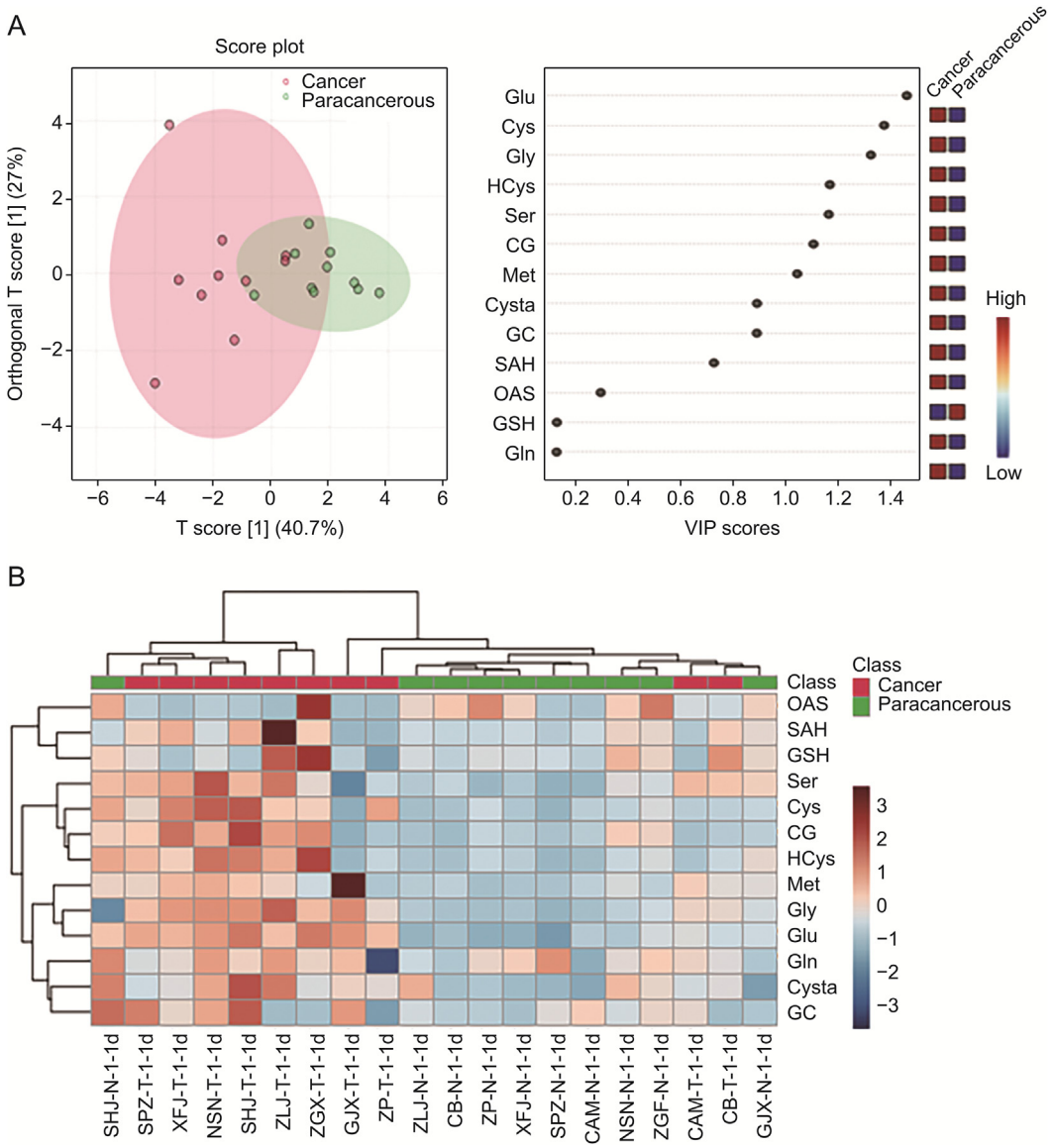

Fig. 7. Difference in the glutathione anabolic pathway (GAP) between the carcinoma and para-carcinoma tissues of esophageal squamous cell carcinoma (ESCC). (A) Score plot of orthogonal partial least squares-discriminant analysis (OPLS-DA) of the carcinoma and para-carcinoma tissues of esophageal squamous cell carcinoma. (B) Heatmap of the relative abundances of the metabolites in each individual patient and hierarchical clustering. Gln: glutamine; Ser: L-serine; Gly: L-glycine; GC: glutamylcysteine; SAH: S-adenylyl homocysteine; Glu: L-glutamine; CG: cysteinylglycine; OAS: O-acetyl-serine; Cys: L-cysteine; Cysta: cystathionine; Hcys: homocysteine; Met: L-methionine; GSH: glutathione.

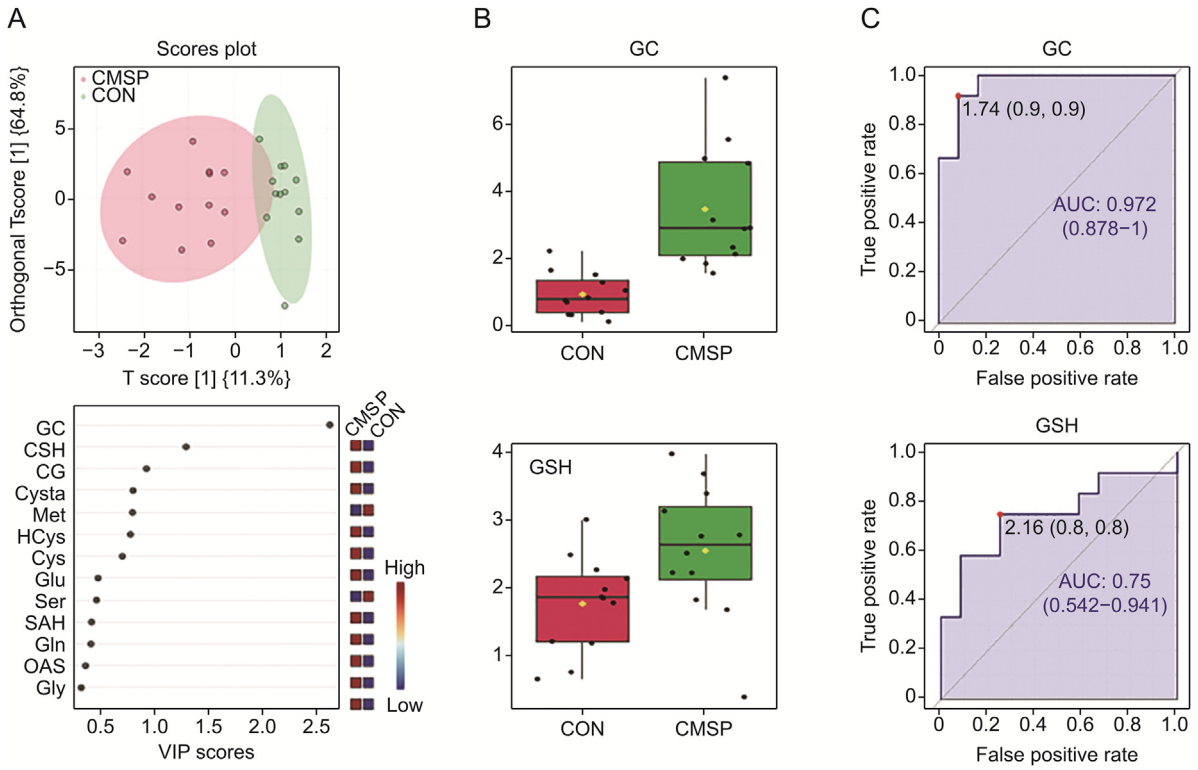

Fig. 8. Effect of CMSP intervention on glutathione anabolic pathway (GAP) in esophageal cancer cells. (A) Orthogonal partial least squares-discriminant analysis (OPLS-DA) scores of the cell administration group and control group. (B) Box plots, and (C) receiver operating characteristic (ROC) curves of the two differential metabolites. CON: control; CMSP: *p*-hydroxycinnamaldehyde; GC: glutamylcysteine; GSH: glutathione; AUC: area under curve.

As shown in Fig. 8, the OPLS-DA model was used to analyze the administration group and the control group, and an obvious separation trend was found among different groups. The VIP values > 1 of GSH and GC were significantly different metabolites in this model. The results of the box diagram showed that the expression levels of GSH and GC in esophageal squamous cells after administration were higher than those in the control group. According to ROC curve analysis, the AUC values of the two compounds were also greater than 0.7, and the AUC value of GC even reached 0.97. Although CMSP can interfere with the production of GSH and GC in cells, the experimental results showed that CMSP exhibits a more significant effect on the expression of GC.

To verify the accuracy of the assessment, differences in the expression of genes regulating glutathione synthesis and metabolism, including glutamate-cysteine ligase catalytic subunit gene (GCLC), glutamate-cysteine ligase modifier subunit gene (GCLM), glutathione synthetase (GSS), and γ-glutamyl transferase (GTT), were detected by reverse-transcription-polymerase chain reaction (RT-PCR). The GCLC and GCLM genes controlling GC synthesis were significantly up-regulated under CMSP intervention, while GSS and GTT were not significantly changed. This was consistent with the results obtained from the glutathione metabolic profile (Fig. S13). When all the data was integrated, it was observed that CMSP could affect the expression of the GCLC and GCLM genes in esophageal cancer cells and thus significantly affect the concentration of GC. As a key precursor compound of GSH synthesis, GC could also promote the up-regulation of intracellular GSH concentration when the expression of the GSS gene did not change significantly. In addition, the GTT gene, which controls the enzymatic hydrolysis of GSH, was not significantly changed after administration and might also cause GSH to accumulate intracellularly.

4. Conclusion

In this study, an effective DMMIC derivatization-assisted LC-MS method was developed for metabolite profiling of GAP in cancer tissues and cells. DMMIC was used as a reagent to label the amino group of metabolites and DTT was used as a reductant to stabilize the thiol group. When DMMIC was combined with LC–MS, the 13 main metabolites on the GAP in complex biological samples could be feasibly quantified. Through systematic methodology evaluation, the developed method was demonstrated to exhibit good linearity (R^2 = 0.9981–0.9999), precision (interday precision of 1.6%–19.0% and intraday precision of 1.4%–19.8%), and accuracy (83.4%–115.7%). Moreover, recovery assessments in tissues (82.5%–107.3%) and in cells (98.1%–118.9%) with GSH-^{13}C2, ^{15}N and Cys-^{15}N demonstrated the reliability of the method in the detection of biological samples.

The method was applied to investigate differences in the GAP between the carcinoma and para-carcinoma tissues of ESCC, as well as the effect of CMSP on the pathway in KYSE-150 esophageal cancer cells. In the former case, the amounts of Glu, Cys, Gly, HCys, Ser, and Met, among the 13 main metabolites of GAP in the carcinoma tissues of ESCC were significantly higher than those in the para-carcinoma tissues, which indicated that upstream glutathione synthesis was activated in the cancer tissue. In the latter case, CMSP affected the expression of GCLC and GCLM genes in KYSE-150 esophageal cancer cells and thus interfered with the synthesis of GC in cells. As a key precursor compound for GSH synthesis, GC can also promote the up-regulation of intracellular GSH concentration without significant changes in GSS gene expression. As the glutathione pathway induces cancer cell death, CMSP may trigger the oxidative stress response of cancer cells and lead to cancer cell death.

In summary, a profiling method to achieve full coverage of the metabolites of GAP was developed. By monitoring the changes in

each node in the metabolic pathway, the pathologic mechanisms of diseases including cancer and neurodegenerative diseases can be studied. The developed method is expected to offer a promising new tool to help researchers elucidate the roles of GAP in physiological and pathological processes.

CRediT author statement

Li Liu: Conceptualization, Methodology, Investigation, Writing - Original draft preparation; **Yu-Han Lu:** Conceptualization, Methodology, Investigation, Writing - Original draft preparation; **Min-Dan Wang:** Methodology, Formal analysis, Investigation; **Qun-Fei Zhao:** Methodology, Investigation; **Xiu-Ping Chen:** Conceptualization, Methodology, Investigation, Resources, Writing - Reviewing and Editing; **Hang Yin:** Conceptualization, Methodology, Investigation, Resources, Writing - Reviewing and Editing; **Chen-Guo Feng:** Supervision, Conceptualization, Funding acquisition, Writing - Reviewing and Editing; **Fang Zhang:** Supervision, Conceptualization, Funding acquisition, Writing - Reviewing and Editing.

Declaration of competing interest

The authors declare that there are no conflicts of interest.

Acknowledgments

We thank the Shanghai Municipal Committee of Science and Technology (Grant Nos.: 20XD1423400, 23ZR1460900 and 20DZ2201100), Shanghai Municipal Health Commission/Shanghai Municipal Administration of Traditional Chinese Medicine (Grant No.: ZY(2021–2023)-0501), Shanghai Science and Technology Development Fund from Central Leading Local Government (Grant No.: YDZX20223100001004), National Natural Science Foundation of China (Grant No.: 21672249), and Expenditure Budget Program of Shanghai University of Traditional Chinese Medicine (Grant Nos.: 2020LK051, and 2021LK001).

Appendix A. Supplementary data

Supplementary data to this article can be found online at https://doi.org/10.1016/j.jpha.2023.08.016.

References

[1] S.C. Lu, Glutathione synthesis, Biochim. Biophys. Acta 1830 (2013) 3143–3153.
[2] L. Wang, Y.J. Ahn, R. Asmis, Sexual dimorphism in glutathione metabolism and glutathione-dependent responses, Redox Biol. 31 (2020), 101410.
[3] N.M. Reddy, S.R. Kleeberger, J.H. Bream, et al., Genetic disruption of the Nrf2 compromises cell-cycle progression by impairing GSH-induced redox signaling, Oncogene 27 (2008) 5821–5832.
[4] H. Kurniawan, D.G. Franchina, L. Guerra, et al., Glutathione restricts serine metabolism to preserve regulatory T cell function, Cell Metabol. 31 (2020) 920–936.e7.
[5] Y. Sun, Y. Zheng, C. Wang, et al., Glutathione depletion induces ferroptosis, autophagy, and premature cell senescence in retinal pigment epithelial cells, Cell Death Dis. 9 (2018), 753.
[6] I. Rebrin, R.S. Sohal, Pro-oxidant shift in glutathione redox state during aging, Adv. Drug Deliv. Rev. 60 (2008) 1545–1552.
[7] M. Vairetti, L.G. Di Pasqua, M. Cagna, et al., Changes in glutathione content in liver diseases: An update, Antioxidants 10 (2021), 364.
[8] C. Espinosa- Díez, V. Miguel, S. Vallejo, et al., Role of glutathione biosynthesis in endothelial dysfunction and fibrosis, Redox Biol. 14 (2018) 88–99.
[9] D. Matuz-Mares, H. Riveros-Rosas, M.M. Vilchis-Landeros, et al., Glutathione participation in the prevention of cardiovascular diseases, Antioxidants 10 (2021), 1220.
[10] Y. Yang, L. Li, Q. Hang, et al., γ-glutamylcysteine exhibits anti-inflammatory effects by increasing cellular glutathione level, Redox Biol. 20 (2019) 157–166.
[11] T.W. Mak, M. Grusdat, G.S. Duncan, et al., Glutathione primes T cell metabolism for inflammation, Immunity 46 (2017) 675–689.
[12] A.V. Ferreira, V.A.C.M. Koeken, V. Matzaraki, et al., Glutathione metabolism contributes to the induction of trained immunity, Cells 10 (2021), 971.
[13] A.K. Elshorbagy, H. Refsum, A.D. Smith, et al., The association of plasma cysteine and γ-glutamyltransferase with BMI and obesity, Obesity 17 (2009) 1435–1440.
[14] H.Q. Li, S.N. Xia, S.Y. Xu, et al., γ-Glutamylcysteine alleviates ischemic stroke-induced neuronal apoptosis by inhibiting ROS-mediated endoplasmic reticulum stress, Oxid. Med. Cell. Longev. (2021), 2961079.
[15] M. Smeyne, R.J. Smeyne, Glutathione metabolism and Parkinson's disease, Free Radic. Biol. Med. 62 (2013) 13–25.
[16] G. Bjørklund, M.D. Doşa, M. Maes, et al., The impact of glutathione metabolism in autism spectrum disorder, Pharmacol. Res. 166 (2021), 105437.
[17] G. Asantewaa, I.S. Harris, Glutathione and its precursors in cancer, Curr. Opin. Biotechnol. 68 (2021) 292–299.
[18] C. Gorrini, T.W. Mak, Glutathione metabolism: an Achilles' heel of ARID1A-deficient tumors, Cancer Cell 35 (2019) 161–163.
[19] M. Luo, L. Shang, M.D. Brooks, et al., Targeting breast cancer stem cell state equilibrium through modulation of redox signaling, Cell Metabol. 28 (2018) 69–86.e6.
[20] H. Ogiwara, K. Takahashi, M. Sasaki, et al., Targeting the vulnerability of glutathione metabolism in ARID1A-deficient cancers, Cancer Cell 35 (2019) 177–190.e8.
[21] S.C. Lu, Regulation of glutathione synthesis, Mol. Aspect. Med. 30 (2009) 42–59.
[22] A. Bansal, M.C. Simon, Glutathione metabolism in cancer progression and treatment resistance, J. Cell Biol. 217 (2018) 2291–2298.
[23] A. Potęga, M. Kosno, Z. Mazerska, Novel insights into conjugation of antitumor-active unsymmetrical bisacridine C-2028 with glutathione: characteristics of non-enzymatic and glutathione S-transferase-mediated reactions, J. Pharm. Anal. 11 (2021) 791–798.
[24] L. Rastogi, K. Dash, J. Arunachalam, Accurate quantitation standards of glutathione via traceable sulfur measurement by inductively coupled plasma optical emission spectrometry and ion chromatography, J. Pharm. Anal. 3 (2013) 180–186.
[25] L. Chen, B.B. Sun, T. Wang, et al., Cigarette smoke enhances beta-defensin 2 expression in rat airways via nuclear factor-B activation, Eur. Respir. J. 36 (2010) 638–645.
[26] S. Ding, G. Feng, Smart probe for rapid and simultaneous detection and discrimination of hydrogen sulfide, cysteine/homocysteine, and glutathione, Sensor. Actuator. B 235 (2016) 691–697.
[27] X.L. Liu, L.Y. Niu, Y.Z. Chen, et al., A multi-emissive fluorescent probe for the discrimination of glutathione and cysteine, Biosens. Bioelectron. 90 (2017) 403–409.
[28] Z. Liu, X. Zhou, Y. Miao, et al., A reversible fluorescent probe for real-time quantitative monitoring of cellular glutathione, Angew. Chem. Int. Ed. 56 (2017) 5812–5816.
[29] H. Malaeb, I. Choucair, Z. Wang, et al., Stable isotope dilution mass spectrometry quantification of hydrogen sulfide and thiols in biological matrices, Redox Biol. 55 (2022), 102401.
[30] S. Li, Z. Lu, L. Jiao, et al., Quantitative determination of D_4-cystine in mice using LC–MS/MS and its application to the assessment of pharmacokinetics and bioavailability, J. Pharm. Anal. 11 (2021) 580–587.
[31] S. Zhao, L. Li, Chemical derivatization in LC–MS-based metabolomics study, Trac. Trends Anal. Chem. 131 (2020), 115988.
[32] A. Roland, R. Schneider, Development and validation of a high-throughput analysis of glutathione in grapes, musts and wines by stable isotope dilution assay and LC–MS/MS, Food Chem. 177 (2015) 152–157.
[33] L. Liu, G.Y. Bao, S.S. Zhang, et al., Analysis of the amine submetabolome using novel isotope-coded pyrylium salt derivatization and LC–MS: herbs and cancer tissues as cases, Anal. Chem. 94 (2022) 17606–17615.
[34] K. Kuwajima, M. Ikeguchi, T. Sugawara, et al., Kinetics of disulfide bond reduction in α-lactalbumin by dithiothreitol and molecular basis of superreactivity of the Cys6-Cys120 disulfide bond, Biochemistry 29 (1990) 8240–8249.
[35] S. Park, I. Hwang, M. Shong, et al., Identification of genes in thyrocytes regulated by unfolded protein response by using disulfide bond reducing agent of dithiothreitol, J. Endocrinol. Invest. 26 (2003) 132–138.
[36] A.L. Harvey, W.F. Dryden, The effect of disulphide bond reduction on cholinoreceptors in cultured skeletal muscle, Biochem. Pharmacol. 23 (1974) 3093–3097.
[37] J. Ferlay, H.R. Shin, F. Bray, et al., Estimates of worldwide burden of cancer in 2008: GLOBOCAN 2008, Int. J. Cancer 127 (2010) 2893–2917.
[38] L. Peng, R. Linghu, D. Chen, et al., Inhibition of glutathione metabolism attenuates esophageal cancer progression, Exp. Mol. Med. 49 (2017), e318.
[39] X. Xu, C. Luo, B. Cao, et al., A potential anti-tumor herb bred in a tropical fruit: insight into the chemical components and pharmacological effects of momordicae *semen*, Molecules 24 (2019), 3949.
[40] L. Zhao, G. Sun, L. Han, et al., P-hydroxycinnamaldehyde induces B16-F1 melanoma cell differentiation via the RhoA-MAPK signaling pathway, Cell. Physiol. Biochem. 38 (2016) 2247–2260.